

## TRANSVERSE-LONGITUDINAL COUPLING IN AN INTENSE ELECTRON BEAM

J.R. Harris<sup>#</sup>, Lawrence Livermore National Laboratory, Livermore, CA 94551, U.S.A.  
R.B. Feldman and P.G. O'Shea, University of Maryland, College Park, MD 20740, U.S.A

### Abstract

This paper describes the longitudinal expansion of a 10 keV, 100 mA electron beam in the University of Maryland Electron Ring. The expansion of the beam tail was found to be sensitive to the choice of transverse focusing settings due to the presence of an abnormality in the beam current profile. Expansion of the beam head, where no abnormality was observed, is in good agreement with the one-dimensional cold fluid model.

### INTRODUCTION

Advanced accelerator applications increasingly require high quality charged particle beams in which the dynamics are governed by space charge. Heavy ion fusion poses a particular challenge as it requires very intense beams to be transported over long distances without reduction in beam quality. A number of longitudinal effects are of particular interest for such applications, including space charge wave propagation [1] and transverse-longitudinal coupling [2]. These and similar effects are being investigated using the University of Maryland Electron Ring (UMER), a strong-focusing, 10 keV, 100 mA electron recirculator for beam physics research [3,4]. In this article, we report experimental evidence for an unexpected transverse-longitudinal coupling in UMER.

### THEORY

Unless contained by longitudinal focusing, an intense initially-rectangular electron beam will evolve longitudinally by expansion from the beam head and tail, which can be calculated using the one-dimensional cold fluid model (Fig. 1) [5]. This expansion is driven by the longitudinal electric field [6]

$$E_z = -\frac{g}{4\pi\epsilon_0\gamma^2} \frac{\partial\lambda}{\partial z}, \quad (1)$$

where  $\epsilon_0$  is the permittivity of free space,  $\gamma$  is the relativistic factor,  $\lambda$  is the local line charge density,  $z$  is the direction along the axis of the beam, and

$$g = \alpha + 2 \ln\left(\frac{b}{a}\right) \quad (2)$$

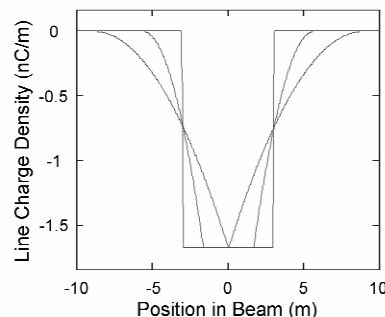


Figure 1: Line charge density profiles for an expanding 10 keV, 100 mA beam in UMER with initial length of 10 ns, calculated from the cold fluid model.

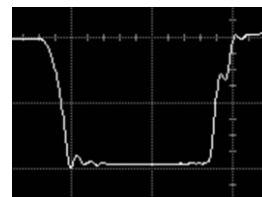


Figure 2: Longitudinal current profile for expanding 100 mA beam in UMER, measured with BPMs. Note similarity of beam head (left) to curves shown in Fig. 1, and current step in beam tail (right). Horizontal scale is 50 ns/div, vertical scale is 50 mA/div

is a geometry factor depending on the beam radius  $a$ , the beam pipe radius  $b$ , and a constant  $\alpha$  which is generally taken to be zero for intense beams and one for emittance-dominated beams [7]. Eq. (1) assumes long-wavelength density variations in a circular beam on axis in a conducting pipe. Driven by the longitudinal electric field, the length of the reduced-density regions at the beam head and beam tail will expand according to

$$z_H = \frac{3c_0 s}{c\beta}, \quad (3)$$

where  $s$  is the distance traveled along the beam line,  $c\beta$  is the beam velocity, and

$$c_0 = \sqrt{\frac{qg\lambda_0}{4\pi\epsilon_0 m\gamma^5}} \quad (4)$$

is the "sound speed" in the electron beam, which depends on the electron charge  $q$  and mass  $m$ , the geometry factor, and the initial line charge density  $\lambda_0$  in the beam flat top [5]. Note that the geometry factor appears in all of these expressions, and is therefore a mechanism for coupling the transverse dynamics (beam radius) into the longitudinal dynamics. Changes in transverse focusing

<sup>#</sup>harris89@llnl.gov

strength or beam current will alter the average beam radius, and will therefore have an effect on the beam's longitudinal expansion. In previous experiments, we investigated the dependence of the geometry factor on beam current in the presence of fixed transverse focusing [2,8]. Although changing the beam current without changing the transverse focusing will result in mismatch oscillations (in addition to the breathing-mode oscillations already present), it was found that the geometry factor could be calculated over a wide range of beam currents by estimating the average beam radius from the transverse envelope equation, assuming smooth transverse focusing.

### EXPERIMENTAL RESULTS

To investigate the sensitivity of the longitudinal dynamics to the choice of transverse focusing settings for a given beam current, the longitudinal expansion of a 100 mA beam was observed as it propagated through UMER under two different transverse focusing solutions [8]. Phosphor screens and cameras located along the beamline were used to record the time-integrated transverse beam profile, and image analysis software written for this experiment was used to extract the vertical and horizontal RMS beam sizes from these images. This data is presented for the two matching solutions in Figs. 3 and 4. Note that we have no information on transverse beam size at locations between phosphor screens. The beam's longitudinal current profile was also measured at a number of positions along the beamline using fast current transformers and capacitive beam position monitors (BPMs) [9]. The 80%-20% rise time for the beam head (Figs. 5 and 6) and tail (Figs. 7 and 8) were extracted from these measurements. The 80%-80% beam length and the 20%-20% beam length were also determined but are not presented here. The error bars are  $\pm 0.7$  ns, which is a conservative estimate based on the oscilloscope sampling rate [8].

The solid and dashed lines in Figs. 5 - 8 are theoretical projections for the rise times calculated from the cold fluid model and given by [8]

$$\tau_{80-20}(s) = \frac{3(0.447)c_0s}{c^2\beta^2}. \quad (5)$$

The projections were calculated both for  $\alpha = 0$  (solid lines) and  $\alpha = 1$  (dashed lines). To calculate the geometry factor from eq. (2), a single beam radius must be determined from the data shown in Figs. 3 and 4 for each matching solution. This was done by summing the average RMS beam size in  $x$  and  $y$  for each matching solution. This is appropriate because it yields twice the average RMS beam size, which is equal to the equivalent hard-edge radius for a beam with uniform transverse density [6], which is approximately true for UMER.

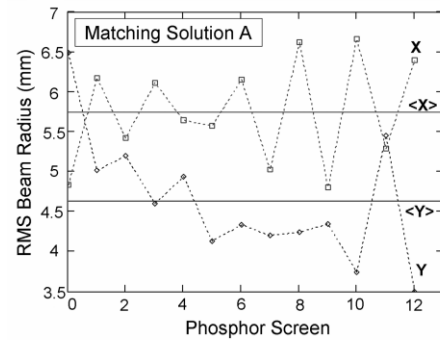


Figure 3: Measured (X,Y) and averaged (<X>,<Y>) beam size for matching solution A.

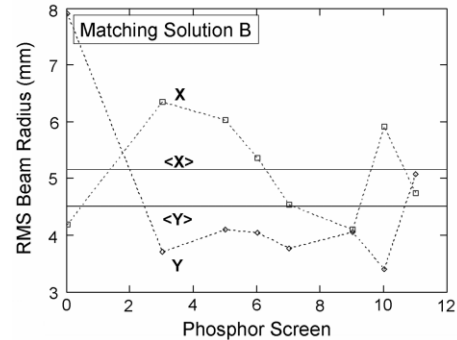


Figure 4: Measured (X,Y) and averaged (<X>,<Y>) beam size for matching solution B.

The results for the beam head and the 80%-80% beam length show very good agreement with the theoretical projections. However, the results for the beam tail and the 20%-20% beam length show much worse agreement, and the pattern of data points is different for each matching solution. This suggests that something is different about the low-current region of the beam tail. Beam profile measurements frequently showed a noticeable step in the beam current at this location (Fig. 2). The behavior of this step is not fully understood at this time. Its source is believed to be in UMER's gridded electron gun [8,10], since the grid bias voltage has been found to affect its strength. However, the step is not seen in the current profile until after the beam has traveled approximately 4 m. This is consistent with the onset of the anomalous data points in Figs. 7 and 8. Also, the BPMs used on UMER have four plates arranged around the beam. When the step was observed, it was not observed equally on all BPM channels. In some cases the step was very visible on one channel and totally absent on another channel at the same BPM. This suggests that a transverse "sloshing" or "wagging" of charge is occurring within the beam tail, in the form of changes in beam shape, density, or both.

To verify that the anomalies seen in the beam tail data are associated with the step, data points were marked if a step was seen in the BPM data at that location (Figs. 7 and 8). Broken circles indicate that a step was seen, but not on the BPM channel used to measure the rise time; solid circles indicate that a step was seen, and was present

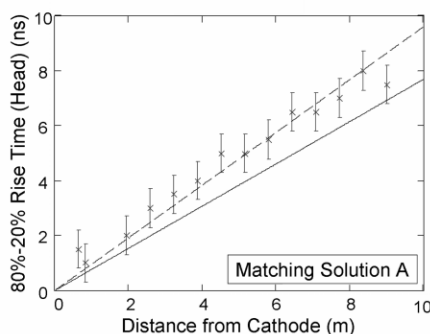


Figure 5: Beam head expansion for matching solution A.

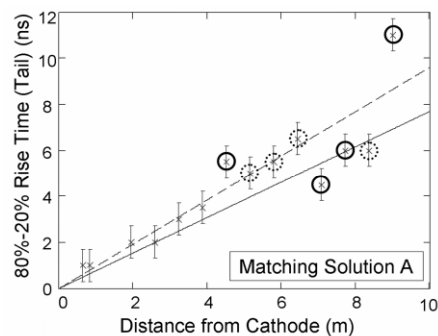


Figure 7: Beam tail expansion for matching solution A.

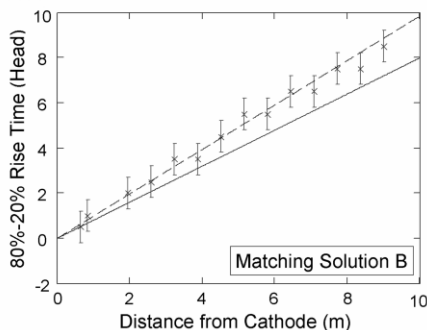


Figure 6: Beam head expansion for matching solution B.

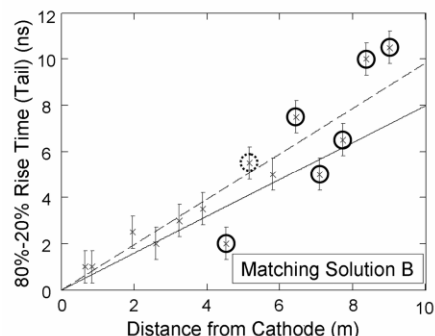


Figure 8: Beam tail expansion for matching solution B.

on the channel used to measure the rise time; and no circle indicates that no step was seen on any channel. In each case where no step was observed on any channel, the rise time was in good agreement with eq. (5). In cases where the step was observed on the channel used to measure the rise time, the measurements did not agree well with eq. (5). And in most of the cases where the step was observed on a channel not used for measuring the rise time, the measurements agreed well with eq. (5) using  $\alpha = 1$ . The differences between Figs. 7 and 8 indicate that the presence of the step on a particular BPM channel and its effect on the length of the beam tail are sensitive to the choice of transverse focusing settings.

## CONCLUSIONS

In this paper, we discussed measurements of the longitudinal evolution of a 100 mA, 10 keV electron beam propagating in a quadrupole focusing channel. To investigate the sensitivity of the longitudinal expansion to the transverse focusing, two different transverse focusing settings were used, and the results compared with the one-dimensional cold fluid model. The model agreed well with the observed evolution of the beam head, but not with the evolution of the beam tail. This was because of a current artifact observed in the beam tail. Although this artifact is believed to be generated in the gridded electron gun used to produce the beam, it is not observed until the beam has traveled approximately 4 m. After that time, its strength, its transverse position on the beam, and its effect on the beam tail rise time are all sensitive to the choice of the transverse matching solution used. This suggests the existence of an unexpected transverse-longitudinal coupling effect in the UMER beam.

## ACKNOWLEDGEMENTS

The authors would like to thank S. Bernal and M. Walter for use of their transverse matching solutions. This research was supported by the Department of Energy, the Office of Naval Research, and the Directed Energy Professional Society. This paper was prepared under the auspices of the U.S. Department of Energy by the University of California, Lawrence Livermore National Laboratory under contract W-6405-Eng-48.

## REFERENCES

- [1] K. Tian, et al., Phys. Rev. ST Accel. Beams **9**, 014201 (2006).
- [2] J.R. Harris, et al., Proc. 2005 Part. Accel. Conf.
- [3] R.A. Kishek, et al., Nucl. Instrum. Meth. Phys. Res. A **544**, 179-186 (2005).
- [4] R.A. Kishek, et al., these proceedings.
- [5] A. Faltens, E.P. Lee, and S.S. Rosenblum, J. Appl. Phys. **61** (12), 15 June 1987, p. 5219.
- [6] M. Reiser, Theory and Design of Charged Particle Beams, Wiley: New York (1994).
- [7] I. Haber, Personal Communication.
- [8] J.R. Harris, Doctoral Dissertation, University of Maryland (2005). Online: [hdl.handle.net/1903/2906](http://hdl.handle.net/1903/2906)
- [9] B. Quinn, et al., Proc. 2003 Part. Accel. Conf.
- [10] I. Haber, et al., Nucl. Instrum. Meth. Phys. Res. A **519**, 396-404 (2004).